



# DALHOUSIE UNIVERSITY

Retrieved from DalSpace, the institutional repository of  
Dalhousie University

<http://hdl.handle.net/10222/80542>

Version: Post-print

**Publisher's version:** Corkum AG, Damjanac B, Lam T. (2018) Variation of horizontal in situ stress with depth for long-term performance evaluation of the Deep Geological Repository project access shaft. *International Journal of Rock Mechanics and Mining Sciences* 107:75–85. <https://doi.org/10.1016/j.ijrmms.2018.04.035>

# Manuscript Submission

1  
2 **Journal:**

3 **International Journal of Rock Mechanics and Mining Sciences**

4  
5 **Title:**

6 **Variation of Horizontal In Situ Stress with Depth for Long-Term**  
7 **Performance Evaluation of the [Deep Geological Repository Project](#)**  
8 **Access Shaft**

9  
10 **Authors:**

11 AG Corkum<sup>a</sup>  
12 B Damjanac<sup>b</sup>  
13 T Lam<sup>c</sup>

14  
15 **Affiliations:**

16 <sup>a</sup> Dalhousie University, Halifax, Nova Scotia, Canada

17 ([andrew.corkum@dal.ca](mailto:andrew.corkum@dal.ca))

18 <sup>b</sup> Itasca Consulting Group, Inc., Minneapolis, Minnesota, USA

19 ([branko@itascacg.com](mailto:branko@itascacg.com))

20 <sup>c</sup>Nuclear Waste Management Organization

21 ([TLam@nwmn.ca](mailto:TLam@nwmn.ca))

22  
23 **Corresponding Author:**

24 AG Corkum

25 Mailing Address:

26 Civil and Resource Engineering

27 Dalhousie University

28 1360 Barrington St.

29 Rm D215, PO Box 15000

30 Halifax, Nova Scotia B3H 4R2

31 Canada

32 Phone: +1 (902) 494-3960

33 Fax: +1 (902) 494-3108

34 Email: [andrew.corkum@dal.ca](mailto:andrew.corkum@dal.ca)

35  

This is a manuscript submitted to the journal for publication consideration. The published version can be obtained directly through the publisher. This should be cited as follows:

Corkum AG, Damjanac B, Lam T (2018) Variation of horizontal in situ stress with depth for long-term performance evaluation of the Deep Geological Repository project access shaft. International Journal of Rock Mechanics and Mining Sciences 107:75–85. <https://doi.org/10.1016/j.ijrmms.2018.04.035>

36 **Research Highlights**

- 37 • A literature review of compiled in situ stress data for Ontario, Canada is presented
- 38 • Variation in geological formation stiffness impacts horizontal stresses
- 39 • A simplified *FLAC3D* model was developed to account for the stratigraphic profile
- 40 • Model calibrated by borehole breakouts, stress measurements and observations
- 41 • An improved estimate of the horizontal stress profile was developed

42

43 **Abstract**

44 A site characterization program was carried out for a proposed Deep Geological  
45 Repository (DGR) project for Ontario Power Generation's (OPG) low- and intermediate-  
46 level nuclear waste repository near Kincardine, ON. The repository is proposed to be  
47 constructed at approximately 680 m below ground surface within the competent  
48 argillaceous limestone of the Cobourg Formation. The in situ stress state at the project site  
49 will have significant impact on both the short- and long-term performance of repository  
50 openings, such as emplacement caverns and access shafts. As part of the site  
51 characterization program, an evaluation of the in situ stress state of the project site was  
52 conducted which consisted, primarily, of a review and synthesis of existing stress  
53 measurements conducted at various locations throughout Ontario and the midwestern U.S.  
54 A summary of the results of past in situ stress studies available in the literature that were  
55 utilized for project "scoping study" level analysis is presented. These past studies,  
56 however, do not account for the impact of the known variation of stress due to  
57 contrasts in stiffness of discrete rock units. This simplification may result in  
58 significant miscalculation of the estimated in situ stress condition. Based on geomechanics  
59 data from deep boreholes and stress measurement data, a simplified FLAC3D model of the  
60 full stratigraphic profile was developed and used to simulate the influence of regional  
61 tectonic strain in the project area. In particular, this method takes into account the rock  
62 properties, such as stiffness, for discrete units at the DGR site. The model was calibrated  
63 on the basis of in situ stresses measured at Norton Mine, in a similar geological  
64 environment as the DGR site, and with site-specific borehole televiewer observations (i.e.,  
65 breakouts). The model-predicted horizontal in situ stress profile showed general agreement  
66 with the observations and also showed the significant influence of discrete rock unit  
67 stiffness.

68 **Keywords:** in situ stress; shaft; *FLAC3D*; long-term performance; nuclear waste  
69 isolation

## 70 **1.0 Introduction**

71 Ontario Power Generation (OPG) is evaluating development of a Deep Geological  
72 Repository (DGR) for long-term storage of Low- and Intermediate-Level Nuclear Waste  
73 (L&ILW) at the Bruce nuclear site near Kincardine, ON. The repository is proposed to be  
74 constructed at approximately 680 m below ground surface (mBGS) within the competent  
75 argillaceous limestone of the Cobourg Formation. A conceptual illustration of the  
76 proposed DGR is shown in Fig. 1. In support of this project, numerous geoscience and  
77 engineering studies have been carried out as part of a site characterization program. A  
78 detailed description of these studies is summarized in Intera [1] and NWMO [2].

79 From a rock mechanics engineering perspective, one of the key challenges is the  
80 determination of contemporary ground stresses at the DGR project site. In situ stresses are  
81 influenced by several factors, the most dominant being: tectonic strain, glaciotectonics and  
82 isostatic rebound, [regional and local structural geology](#), deposition and erosion, and  
83 topography. Moreover, the geological history associated with these events is also a major  
84 factor. As a result, the stress regime can be complex and variable.

85 The stratigraphic profile at the site consists of a near horizontally bedded sequence of  
86 carbonates and shales. The strength and stiffness characteristics of these various discrete  
87 rock units are anticipated to vary significantly. Amadei et al. [3] and Esterhuizen et al.,  
88 [4] have shown that horizontal in situ stresses could be dependent on the stiffness of  
89 discrete rock units. Further to that, these horizontal stresses vary with direction in the  
90 horizontal plane with a *maximum principal horizontal stress* ( $\sigma_H$ ) and *minimum principal*  
91 *horizontal stress* ( $\sigma_h$ ).

92 Currently, there are no in situ stress measurements at the project site. There are great  
93 challenges in obtaining, within suitable confidence levels, the in situ stress magnitude and  
94 orientations at the depth of interest from a surface-based exploratory borehole. This is  
95 particularly the case for the horizontally bedded formations at the Bruce nuclear site as  
96 hydrofracture techniques cannot be used with confidence because the vertical stress is less  
97 than the horizontal stresses [5]. Traditional strain-relief methods, such as overcoring, are  
98 suitable only for relatively shallow measurements and testing within exploration boreholes  
99 at the repository depth has not been successfully demonstrated. Consequently, during the  
100 course of the DGR site characterization program, the state of in situ stress was estimated

101 based on several lines of reasoning including: regional stress data [6-9]; observations made  
102 during drilling and monitoring of the DGR series of vertical boreholes [1]; and the in situ  
103 stress modelling of the sedimentary succession below the site described in this paper.

104 As part of a project to evaluate the long-term performance of shafts and repository  
105 excavation openings [10], the authors have examined in situ stress conditions, in particular  
106 the variation of horizontal stresses due to rock unit stiffness within the sedimentary  
107 sequence. This was done by carrying out a three-dimensional finite difference analysis  
108 model using *FLAC3D* [11] to simulate the tectonic strain within the sedimentary sequence.  
109 The model was calibrated with the site-specific borehole televiewer observations and other  
110 in situ stress observations pertinent to the project site.

111 This paper first presents a review of the in situ stresses from literature followed by the  
112 interpretation of acoustic televiewer data from deep exploration boreholes at the site.  
113 Finally, the in situ stress model analysis (*FLAC3D*) that accounts for the contrasting  
114 stiffness of the various layers is described. The findings from these three approaches are  
115 compared.

## 116 **2.0 Background: In situ Stresses in Southern Ontario**

117 This section presents a brief overview of the geological setting in the project area and  
118 a review of in situ stress measurement compilations carried out for the Southern Ontario  
119 region. The in situ stress measurement carried out at 670 m depth in Norton Mine, Ohio, is  
120 also discussed.

### 121 **2.1 Geological Setting**

122 A summary of the regional site geology of the proposed site is presented by Intera [1].  
123 The NE-SW trending Algonquin Arch separates the Michigan and Appalachian Basins in  
124 Southern Ontario (see Fig. 2). The proposed DGR site is in the eastern portion of the  
125 Michigan Basin within a sequence of sedimentary units of Upper Cambrian to Upper  
126 Devonian age. The sedimentary rocks rest on the southern margin of the Canadian Shield  
127 crystalline basement rocks of the Proterozoic Grenville Province. A stratigraphy profile of  
128 the bedrock at the DGR site based on four deep boreholes is shown in Fig. 3 [1].

## 129 **2.2 Vertical Stresses**

130 It is generally believed that the vertical in situ stress ( $\sigma_v$ ) in the region is comprised of  
131 a simple gravitational gradient based on the density of the rocks within the stratigraphic  
132 section. Given that the sedimentary rocks in the upper approximately 800 m have similar  
133 density, a uniform vertical stress gradient is a suitable approximation for the depths under  
134 consideration for the DGR project. Valley and Maloney [12] proposed:  $\sigma_v = 0.0259z$  (in  
135 MPa): where  $z$  is depth in meters.

## 136 **2.3 Horizontal Stresses**

137 Based on the geological (i.e., tectonic) history of the region, high horizontal stresses  
138 exist and this has been supported by numerous measurements and observations [13]. The  
139 horizontal to vertical principle stress ratios for the maximum horizontal stress ( $K_H = \sigma_H / \sigma_v$ )  
140 and minimum horizontal stress ( $K_h = \sigma_h / \sigma_v$ ) both exceed one. Different horizontal stress  
141 gradients have been reported by several authors, some prepared specifically for the DGR  
142 project, and these are summarized in the following sections.

### 143 **2.3.1 Adams and Bell, 1991**

144 Using overcoring stress measurements in shallow boreholes and workings, and deep  
145 hydraulic fracturing borehole data from Darlington, Ontario, Adams and Bell [6]  
146 demonstrated the high horizontal compressive stress characteristic of the Mid-Plate Stress  
147 Province of Eastern North America. Most of the stress data are measured in the Paleozoic  
148 rock sequence of Southern Ontario which consists of near flat-lying carbonate, shale and  
149 sandstone formations of Ordovician, Silurian and Devonian periods. The state of high  
150 horizontal stress in the rock of this region is primarily the product of major depression of  
151 the area during the Wisconsin Glaciation and subsequent isostatic rebound. Adams and  
152 Bell [6] presented data mostly from Silurian and Ordovician formations while deep  
153 hydraulic fracturing stress values, to depths of just over 300 m in the Precambrian Shield  
154 basement, were measured at Darlington, Ontario by Haimson and Lee [14]. A compilation  
155 of stress measurements in the Precambrian Shield for Northern Ontario was developed by  
156 Kaiser and Maloney [8] and updated by Yong and Maloney [15]. The results from the  
157 former are discussed in the following section.

158 The reported strain relief in situ stress measurements conducted at shallow depths were  
 159 all obtained using USBM (United States Bureau of Mine) borehole deformation gauges.  
 160 The measurements show significant scattering, but provide a general trend for the in situ  
 161 stress gradient with depth. Hydraulic fracturing tests indicated a lower vertical stress  
 162 gradient with depth. Based on these findings, the following expressions of vertical  
 163 horizontal in situ stress with depth were established:

$$164 \quad s_H = 0.027z \text{ (in MPa)} \quad (1)$$

$$165 \quad s_h = 0.017z \text{ (in MPa)} \quad (2)$$

### 166 **2.3.2 Kaiser and Maloney, 2005**

167 Kaiser and Maloney [8] published a review of an in situ stress database for the  
 168 Ontario portion of the Canadian Shield. Much of the shield database was a recompilation  
 169 of an in situ stress database compiled by CANMET Mining and Mineral Sciences  
 170 Laboratories [16]. This study utilized linear regression techniques on overcoring  
 171 measurement data from mines in northern Ontario, subdividing the Shield region into  
 172 various sub-regions and three depth zones or “stress domains” similar to those of  
 173 Canadian and Swedish regions reported by Martin et al. [17].

174 Domain 1 (Stress Relaxed Zone) is a zone influenced by near surface topography,  
 175 weathering, etc. and extends from the ground surface to a depth of approximately  
 176 300 mBGS. Domain 2 (Transition Zone) is a transition zone between Domains 1 and 3. It  
 177 exists between approximately 300 and 600 mBGS. Domain 3 (Maximum Stress Zone or  
 178 Undisturbed Zone) exists below approximately 600 mBGS below ground surface and is a  
 179 region of limited fracturing and minimal impact from surficial conditions.

180 The following in situ stress gradients were recommended for each domain based on  
 181 linear regression of existing measurements. Note that the values in square brackets  
 182 represent the 95% confidence interval limits on the respective component.

#### 183 **Domain 1:**

$$184 \quad s_H = 5.768 [\pm 3.358] + 0.071 [\pm 0.019]z \text{ (in MPa)} \quad (3)$$

$$185 \quad s_h = 3.287 [\pm 2.600] + 0.043 [\pm 0.015]z \text{ (in MPa)} \quad (4)$$

$$186 \quad s_v = 0.034 [\pm 0.005]z \text{ (in MPa)} \quad (5)$$



187 **Domain 3:**

188  $s_H = 23.636 [\pm 11.556] + 0.026 [\pm 0.012]z$  (in MPa) (6)

189  $s_h = 17.104 [\pm 10.538] + 0.016 [\pm 0.010]z$  (in MPa) (7)

190  $s_v = 1.066 [\pm 8.247] + 0.020 [\pm 0.008]z$  (in MPa) (8)

191 **Domain 2:** The transition zone can be described by a linear construction between  
192 Domain 1 and Domain 3. Variability and uncertainty is high in this transitional stress  
193 domain.

194 Yong and Maloney [15] provided an update to the 2005 database and the domains  
195 using 75 new measurements since 2005. This new dataset covers measurements ranging  
196 from depths between 12 and 2,552 m. A data screening process was also performed to  
197 assess quality and reduce uncertainty when establishing representative ground stress state  
198 equations. The state of ground stress was found to be consistent with the 2005 study,  
199 subdividing into the same three domains.

### 200 **2.3.3 Lam et al., 2007**

201 Lam et al. [7] carried out a review of the available stress data in the Paleozoic rocks  
202 measured from over 20 sites in the lower Great Lakes Region. These measurements were  
203 primarily made using overcoring methods (mostly at shallow depths with several at about  
204 700 m in the Norton Mine, Ohio) and by hydraulic fracturing to depths of 5,100 m in central  
205 Michigan State. They were made in various rock types such as shale, carbonate and  
206 sandstone. The analysis of the regional ground stress data allows for an estimate of the  
207 approximate range of stress ratios at the repository depth under consideration. On the basis  
208 of this review, the following recommended stress ratios were proposed for the DGR  
209 project:  $\sigma_H/\sigma_v = 2.0$  to  $2.5$  and  $\sigma_h/\sigma_v = 1.5$ . Assuming a uniform density of  $2600 \text{ kg/m}^3$  for  
210 the stratigraphic units over the depth of interest, these stress ratio values can be converted  
211 to the following stress gradients:

212  $s_H = 0.051z$  to  $0.064z$  (in MPa) (9)

213  $s_h = 0.038z$  (in MPa) (10)

214 **2.3.4 Horizontal Stress Orientation**

215 An excerpt from the World Stress Map project [18] shows the locations of stress  
216 measurements and stress indicators (e.g., borehole breakouts) in Southern Ontario and the  
217 Mid-Western U.S. in Fig. 4. There are no measurements or direct observations mapped  
218 within approximately 200 km of the DGR site prior to drilling the DGR deep boreholes at  
219 Bruce nuclear site in 2007. Based on the mapped stress orientations, there is some  
220 variability in orientations in the Ottawa-Quebec City region (St. Lawrence Lowlands). In  
221 the remainder of the map area, the stress orientation indicators are consistent and indicate  
222 an *ENE-WSW* major principle stress orientation. This regional orientation was also  
223 presented by most other researchers [6-9]. This general trend was confirmed by ellipticity  
224 detection analyses using acoustic televiewer logs from four DGR deep boreholes [2]. Given  
225 the consistency of the stress indicator orientations and the similarity of the geological  
226 setting within the map area, the stress orientation in the DGR area is likely similar to the  
227 general regional trend with an ENE-WSW maximum principle horizontal stress ( $\sigma_H$ )  
228 orientation. The minimum principal horizontal stress ( $\sigma_h$ ) is orthogonally oriented with an  
229 NNW-SSE trend.

230 **2.4 Norton Mine Stress Measurements**

231 The Cobourg Unit is the target formation for the DGR host rock (i.e., storage caverns).  
232 The depth and litho-mechanical variations around the repository horizon are very similar  
233 to those of the Columbus limestone at the Norton Mine near Akron in Ohio. Bauer et al.  
234 [19] described a program of in situ stress measurements that was carried out in the  
235 limestone for evaluation of a proposed compressed air energy storage project. Although  
236 this room-and-pillar limestone mine is located approximately 350 km away, horizontal in  
237 situ stress magnitudes would be controlled by similar stiffness contrasts between  
238 stratigraphic units. The Columbus limestone unit ( $E = 49$  GPa) has mechanical properties  
239 similar to those of the Cobourg limestone ( $E = 37.1$  GPa). Moreover, the two units occur  
240 at similar depths: approximately 670 m for the Columbus Unit and 655 m for the Cobourg  
241 Unit (see Fig. 3).

242 The in situ stress measurement program was carried out in 1999 and 2000 using the  
243 USBM overcoring method. The measurements were made in Drift 9B in an area of the  
244 room-and-pillar mine relatively isolated from other near-by excavations. The authors also

245 pointed out that results agreed with other in situ stress testing in the vicinity using  
246 overcoring and hydrofracturing methods. The recommended in situ stress values from the  
247 program at Norton Mine were:  $\sigma_H = 36.7$  MPa (oriented N75°W);  $\sigma_h = 28.3$  MPa;  $\sigma_v =$   
248 22.5 MPa ( $\sim 1.26 \times$  overburden).

249 The recommended stress values at Norton Mine are substantially higher than  
250 proposed by Adams and Bell, but similar to those proposed by both Lam et al. and Kaiser  
251 and Maloney.

## 252 **2.5 Summary**

253 The vertical and horizontal stress orientations presented in past studies are in close  
254 agreement. However, there is some discrepancy in the proposed horizontal stress  
255 gradients. Fig. 5 shows the maximum ( $\sigma_H$ ) and minimum ( $\sigma_h$ ) horizontal stress gradients  
256 from all authors, along with the measured values from Norton Mine. On this plot the  
257 values from Norton Mine are plotted within the Cobourg Unit, a mechanically  
258 comparable limestone unit at similar depth as the Columbus Limestone where the actual  
259 measurements were made.

260 From the plot in Fig. 5, it can be seen that the Adams and Bell gradient results in the  
261 lowest stress magnitudes while the Kaiser and Maloney tri-linear gradient has the highest  
262 magnitudes above 600 mBGS. The Lam et al. gradients are essentially bounded by the  
263 Adams and Bell (at shallow depth), and the Kaiser and Maloney (at greater depth)  
264 gradients. Below about 600 – 700 mBGS the Lam et al. gradients are the highest stress  
265 magnitudes. Both the Kaiser and Maloney, and the Lam et al. agree well with the  
266 measured values at Norton Mine (within repository horizon). Given the overall  
267 agreement, either of the above predicted gradients seem suitable to be used to develop a  
268 representative ground stress profile.

269 A number of authors [20-22] have recognized the impact of the elastic parameters on  
270 the distribution of horizontal in situ stresses and have verified the observation by  
271 comparison to measured values. Based on an analysis of hydrofracturing results, Swolfs  
272 [23] determined that horizontal stiffness has a significant impact on horizontal stresses.  
273 Horizontal stresses in horizontally bedded sedimentary basins are affected by the  
274 distribution of relative stiffness of the rock units (i.e., stiff sandstone versus soft

275 mudstone). Because of the high contrasting stiffness of stratigraphic units along the  
276 proposed DGR Access Shafts, and the high contrast in situ horizontal stresses, this may  
277 be an important factor in long-term shaft performance.

### 278 **3.0 Borehole Televiewer In Situ Stress Constraints**

279 As part of the site characterization program at Bruce nuclear site, an acoustic televiewer  
280 was used to log the six DGR deep boreholes drilled between 2007 and 2010. This  
281 allowed for estimation of in situ stress magnitudes using observations from borehole wall  
282 conditions (e.g., breakouts), assuming that one principal stress is vertical. The absence of  
283 breakout observed in the boreholes set an upper bound on the allowable maximum  
284 horizontal stress magnitude of the formation. The logs were reviewed to evaluate  
285 borehole wall damage and shape, such as breakouts, tensile fractures and “ovaling.”  
286 Breakouts are zones of failure that occur in the borehole wall where the strength of the  
287 rock is exceeded by the stresses in the borehole perimeter. Often breakouts occur as  
288 diametrically opposed “notches” in the borehole wall. Tensile fractures are sometimes  
289 difficult to distinguish from other structural features in the borehole walls, but are  
290 typically expressed as a steeply dipping parallel family of fractures. Borehole ovaling is  
291 distortion of the circular borehole due to the stress field. Because of their relationship  
292 with borehole stresses, these features are often an indicator of the in situ stress field in the  
293 plane of the borehole. The location of the breakouts and tensile fractures provides an  
294 indication of the orientation of the stress field and, by comparison to the rock strength,  
295 the features provide an indication of the stress magnitude.

296 Valley and Maloney [12] reviewed the televiewer logs and carried out a series of  
297 calculations in order to constrain the likely stress field for the DGR project. The televiewer  
298 logs indicated that no borehole breakouts exist along DGR-1 and DGR-2. The lack of  
299 observed borehole breakouts is a positive sign for shaft performance; however, it limits the  
300 opportunity to evaluate the in situ stress field. While calculation of the stresses exceeding  
301 the rock strength is not suitable in these cases, an analysis can be carried out to determine  
302 the maximum stress conditions that could be present without inducing borehole breakout.  
303 Two zones of tensile fracturing were observed and intervals of borehole ovaling were also  
304 observed.

305 According to Zoback [24], observations and measurements indicate that in situ stresses  
 306 at depth are limited by stress acting on critically oriented discontinuities in the earth's crust  
 307 with strength parameters of zero cohesion and Coefficient of Friction ( $\mu$ ) of 0.6 to 1. For  
 308 borehole excavation-induced stresses  $\sigma'_1$  and  $\sigma'_3$  are the maximum and minimum stresses  
 309 around the borehole calculated elastically, respectively. On the basis of this observation,  
 310 the maximum stress ratio that can exist is limited by:

$$311 \quad \sigma'_1 / \sigma'_3 = \frac{(s_1 - u)}{(s_3 - u)} = [(m^2 + 1)^{1/2} + m]^2 \quad (11)$$

312 Eq. (11) provides one constraint on the in situ stress field in a large-scale context.  
 313 Borehole breakouts provide an additional constraint. In order to compare rock strength with  
 314 borehole televiewer observations, applicable strength parameters were required.  
 315 Laboratory testing data using core samples from DGR-1 and DGR-2 was used to determine  
 316 the applicable formation elastic and strength properties for the formations of interest [12].  
 317 The rock compressive strength can be compared to the maximum tangential stress ( $\sigma_{\theta, max}$ )  
 318 around a borehole wall calculated from:

$$319 \quad s_{q, max} = 3s_H - s_h - u_{bh} - \alpha u \quad (12)$$

320 Where:  $u_{bh}$  borehole fluid pressure;  
 321  $\alpha$  effective stress coefficient for the rock in compression;  
 322  $u$  formation pore pressure.

323 A simplified and conservative model for pore pressure ( $u$ ) was assumed with a  
 324 hydrostatic pore pressure gradient from ground surface:  $u = 9.81z$  in kPa. According to  
 325 Brace and Martin [25],  $\alpha$  is typically close to 1 for low porosity rocks.

326 There is some question as to what is the appropriate measure of rock strength for  
 327 breakout prediction. Typically, the Unconfined Compressive Strength ( $\sigma_c$ ) has been used;  
 328 however, Martin [26] has suggested the Damage Initiation threshold ( $\sigma_{cd}$ ) is a better  
 329 indicator of failure at the borehole scale. More recently, the Crack Initiation threshold ( $\sigma_{ci}$ )  
 330 has been identified as the likely best indicator of the onset of spalling for rock excavations  
 331 [27].

332 Tensile fracturing was also used to constrain the stress field. Tensile failure was  
333 predicted when the tensile strength ( $\sigma_t$ ) was exceeded by the minimum tangential stress  
334 ( $\sigma_{\theta, min}$ ) around the borehole according to:

$$335 \quad s_{q, min} = 2s_h - s_H - u_{bh} - bu \quad (13)$$

336 Where:  $\beta$  effective stress coefficient for the rock in tension.

337 Valley and Maloney [12] stated that as a conservative estimate, it was assumed that  $\sigma_t$   
338 = 0 and  $\beta = 0$ . Although it could be argued that the laboratory-scale tensile strength would  
339 be a more suitable constraint, the condition assumed by the authors is likely a conservative  
340 assumption with respect to the predicted in situ stress bounding conditions.

341 Although a single stress field tensor could not be determined from the calculations,  
342 Eqs. (11), (12) and (13) were used by Valley and Maloney to provide a range of possible  
343 stress conditions. By further adding the rock strength for each unit, the maximum  
344 permissible magnitude of  $\sigma_H$  and minimum permissible magnitude of  $\sigma_h$  could be  
345 determined for the full stratigraphic profile where strength data were determined. Table 1  
346 presents the constrained stress values on the basis of the strength parameter  $\sigma_{ci} = 0.5\sigma_c$ .  
347 These stress values are also shown in Fig. 6.

348 In addition to observations of borehole wall damage, the televiwer data was used to  
349 measure borehole shape, in particular to observe ovaling of the hole. Histograms of  
350 borehole ovaling orientations from televiwer observations are provided in Fig. 7. Valley  
351 and Maloney concluded that systematic SE oriented elongation implied a NE-SW  
352 maximum principal stress orientation ( $\sigma_H$ ). This is in agreement with the estimated  
353 principal horizontal stress orientations proposed by other researchers, as discussed in  
354 Section 2.3.4.

355 The absence of borehole breakouts and minimal observed tensile fractures limit the  
356 applicability of constraining the stress tensor with this exercise. However, as part of a  
357 preliminary evaluation of the in situ stress conditions for the DGR project, these  
358 observations related to in situ stress conditions are a significant benefit to the site  
359 characterization program.

#### 360 **4.0 Modelling Methodology for In Situ Stress Evaluation**

361 In order to develop a three-dimensional *FLAC3D* model that captures the important  
362 aspects of the site stratigraphy without unnecessary complexity, the stratigraphy was  
363 simplified into units of similar mechanical behavior. This simplified model is referred to  
364 as a *Geotechnical Model*. The simplifying assumptions were based on a relative  
365 comparison of the elastic properties of the geological units, the geological/geotechnical  
366 descriptions of the units, and groupings previously proposed by others [12,28].

367 As part of this study the authors synthesized laboratory testing data carried out on  
368 core samples from four boreholes at the DGR site (DGR-1 through DGR-4). The testing  
369 consisted of uniaxial compressive strength, triaxial compressive strength, long-term  
370 compressive strength, and Brazilian testing. In total, data from 176 different laboratory  
371 tests was correlated. Test data were not available for all units in the stratigraphic  
372 sequence. Units where testing was unavailable were grouped with adjacent units of  
373 similar geological description and characteristics. The proposed stratigraphic units and  
374 elastic properties are provided in Table 2. Note that the units are numbered in the table  
375 from 1 – 12 for identification. [Further details regarding the site characterization and](#)  
376 [laboratory testing program can be found in \[1,2,10\].](#)

377 The strength and stiffness characteristics of the various discrete rock units anticipated  
378 to be encountered throughout the sedimentary sequence are expected to vary significantly.  
379 The variation of Young's modulus ranges from about 5 to 75 GPa (a factor of 15) from the  
380 softest to stiffest unit with a similar variation in strength parameters. If a uniform stress  
381 gradient were used to evaluate rock mechanics stability that omits the impact of horizontal  
382 stiffness on stresses, this could result in significantly overestimating damage in soft/weak  
383 rocks and underestimating damage in stiff/strong rocks.

384 The objective of the modelling study was to evaluate the horizontal in situ stresses  
385 while accounting for the stiffness of discrete rock units along the proposed DGR access  
386 shaft's stratigraphy. Three-dimensional variability, such as topography and variation in  
387 geological conditions away from the borehole locations, was not considered in this  
388 modelling exercise. Given these limitations, the issue could be addressed for the site by  
389 developing a simple linear elastic three-dimensional multi-layered solution. An analytical  
390 method to calculate the stress distribution, including the variation of horizontal stress due

391 to the elastic parameters of discrete rock units, was developed by Amadei et al. [3].  
392 However, because a three-dimensional stress analysis model using *FLAC3D* was already  
393 in development to evaluate the DGR access shaft design it was efficient to use a simplified  
394 version of this model to carry out an in situ stress evaluation.

395 Using the finite difference code *FLAC3D*, a very slender single-zone wide (1 m cubic  
396 elements) model was developed that extended vertically from the ground surface to a depth  
397 below ground surface of 1200 m. The model included the 12 geological units listed in Table  
398 2. An elastic constitutive model was used for all zones and the elastic parameters for each  
399 unit is provided in Table 2. In the model, a uniform density of 2600 kg/m<sup>3</sup> was used  
400 throughout the stratigraphic sequence. The model was set up so that the *x*-axis and the *y*-  
401 axis represented the NE-SW and the NW-SE orientations, respectively.

402 The model was executed in two stages: Stage 1 to capture gravitational loading and  
403 Stage 2 to apply tectonic strain. Initially, the model boundary conditions consisted of *roller*  
404 boundaries (i.e., constrained only in the direction normal to the face) on all sides and the  
405 bottom with a *free* boundary at the ground surface. These boundary conditions simulated  
406 lateral symmetry consistent with a large lateral spatial extent. The model was cycled until  
407 *pseudo-static equilibrium* was achieved (i.e., a low ratio of unbalanced forces within the  
408 model relative to the maximum nodal force in the model). At this initial state, the model  
409 was in equilibrium under the zone's body forces (gravitational loading) and the horizontal  
410 stresses in the model were due to Poisson's ratio only. In this state the horizontal stresses  
411 can be approximated by:

$$412 \quad s_H = s_h = gz \frac{n}{1 - n} \quad (14)$$

413 Following the state of initial equilibrium, the next stage was to “squeeze” the model  
414 laterally to simulate the effect of tectonic compression experienced by the sedimentary  
415 basin over geological time scales. The roller boundary conditions were removed from the  
416 positive *x* and positive *y* faces of the model. Constant velocity boundary conditions were  
417 then added to the positive *x* and *y* faces moving them in a compressional direction. The  
418 magnitude of the velocity boundary conditions was set so they moved slow enough so that  
419 the model remained in a state of pseudo-static equilibrium at all times during model  
420 cycling. In order to achieve a suitable ratio of in situ horizontal stresses, the constant



421 velocity boundary conditions were applied in a *velocity ratio* ( $v_H/v_h$ ) equal to the desired  
422 ratio of  $\sigma_H/\sigma_h$ . A schematic illustration of the *FLAC3D* model is shown in Fig. 8.

423 In order to arrive at a *calibrated* model, or a model deemed to reasonably match actual  
424 in situ stress conditions, numerous model simulations were carried out. Models were cycled  
425 with the constant displacement boundary conditions using several velocity ratios and each  
426 simulation was cycled until a close match to the constraining data was achieved. The  
427 resulting stress profile from each simulation was compared to the constraints from the  
428 borehole observations ( $0.5\sigma_c$ ) and the deep stress measurement from Norton Mine. As  
429 mentioned previously, the Cobourg Limestone unit is the target formation for the  
430 repository, as such it was considered particularly important to match the measured stresses  
431 in the Columbus Limestone from Norton Mine.

## 432 **5.0 Model-Predicted Horizontal Stress Gradient**

433 From the various simulations carried out, a good match to the constraining data was  
434 achieved from the *FLAC3D* model with horizontal strains of  $\varepsilon_x = 5.16 \times 10^{-4}$  and  
435  $\varepsilon_y = 2.84 \times 10^{-4}$ . This corresponds to a velocity ratio of 1.82. The horizontal stress profiles  
436 for the calibrated model are shown in Fig. 9 compared with the constraining conditions and  
437 literature-reported gradients. The model results are highly variable, compared to the  
438 literature-reported gradients and illustrates the implications of rock bed stiffness on the  
439 horizontal in situ stresses.

440 Compared to a uniform stress gradient, the model-predicted profile clearly shows  
441 elevated horizontal stresses in Unit 5 (Salina E: 379 – 415 m) and Unit 9 (Cobourg-  
442 Collingwood: 665 – 693 m) units, and the deep Unit 12 (Cambrian and Precambrian: below  
443 848 m). The horizontal stresses were particularly low in Unit 2 (Lucas: 131 – 176 m) and  
444 Unit 7 (Cabot Head: 612 – 656 m). Even more significant than the variation in stresses  
445 across units is the abruptness of the model stress changes along the profile. The horizontal  
446 stresses transitioning between adjacent units can vary up to 100% or more.

447 By comparing the model-predicted horizontal stresses and the literature-reported  
448 gradients shown in Fig. 9, it can be seen that the model-predicted stresses are bound by the  
449 Adams and Bell gradient on the low side, and the Kaiser and Maloney gradient on the high

450 side. In particular, the Adams and Bell gradient shows a better match in the upper 650 m,  
451 while the tri-linear Kaiser and Maloney gradient shows a better match at greater depth. As  
452 mentioned previously, the Lam et al. gradient (shown with the range of values in yellow)  
453 provides a transition between the Adams and Bell, and the Kaiser and Maloney gradients.  
454 The Adams and Bell gradient is based primarily on softer sedimentary rocks in southern  
455 Ontario while the Kaiser and Bell is based on a wider geographical region of the Canadian  
456 Shield including rock units of metamorphic and igneous origin. As a result, model-  
457 predicted stresses in the softer upper sedimentary units tend towards the Adams and Bell  
458 gradient, while the stiffer lower units tend towards the Kaiser and Maloney gradient. The  
459 model results are in good agreement with the literature-reported gradients in addition to  
460 providing a good match to the constraints (Norton Mine measurements and borehole stress  
461 constraints at the Bruce nuclear site).

462 A profile of the in situ stress ratios ( $K_H$  and  $K_h$ ) is plotted in Fig. 10. The corresponding  
463 plot of in situ stress ratios is similar to those presented by other researchers [22] with high  
464 ratios in the upper 100 m and reducing significantly with depth to some stabilized value.  
465 Moreover, the variation of stress ratio relative to discrete bed stiffness is similar to that  
466 proposed by Amadei et al. [3].

467 Long-term performance of the DGR is being evaluated for a period of 1 M years;  
468 therefore, both short- and long-term performance issues were considered. The Access Shaft  
469 numerical modelling-based rock mechanics evaluation accounted for many issues, such as:  
470 excavation, glacial loading, seismic loading, time-dependent degradation of rock and seals  
471 materials and pore pressure evolution [10]. The horizontal in situ stresses likely have the  
472 greatest impact on the long-term time-dependent behaviour of the shaft and seals. For  
473 relatively unjointed rock mass (e.g.,  $GSI > 60$ ), the short-term shaft boundary/wall damage  
474 (e.g., spalling) is dependent on the ratio  $\sigma_{max}/\sigma_c$  [17] where  $\sigma_{max}$  is the maximum tangential  
475 stress calculated elastically around a circular opening.

$$476 \quad s_{max} = 3s_H - s_h \quad (15)$$

477 Based on the findings of Damjanac and Fairhurst [29] deviatoric stress in the rock unit  
478 dominates long-term behaviour which can also be evaluated at the excavation boundary by  
479 the ratio  $\sigma_{max}/\sigma_c$ . Therefore, the magnitude of  $\sigma_{max}$  is critical to shaft performance  
480 prediction.

481 A plot showing the profile of  $\sigma_{max}$  from the model-predicted horizontal stress profiles  
482 and two of the literature-reported gradients, for comparison are presented in Fig. 11.  
483 Accounting for the in situ horizontal stresses due to stiffness of discrete units results in a  
484 significantly different  $\sigma_{max}$  profile and consequently resulting predictions of shaft short-  
485 and long-term performance. Table 3 provides a summary of conditions at Access Shaft seal  
486 locations analyzed for preliminary engineering studies carried out by the authors [10]  
487 showing the geological unit, horizontal stresses, maximum tangential stress, and predicted  
488 ratio of  $\sigma_{max}/\sigma_c$  for each seal analyzed. The units corresponding to specific seal locations  
489 differs, to some extent, from the simplified Geotechnical Model used in modelling for  
490 horizontal stress evaluation. There are some differences in the specific units corresponding  
491 to seal locations, and their associated mechanical properties listed in Table 3, compared to  
492 those of the overall Geotechnical Model presented in Table 2.

493 Although the calibrated model has captured the influence of discrete bed stiffness on  
494 horizontal stresses, there are some notable limitations: most notably, the lack of site-  
495 specific in situ stress measurements for a more direct calibration. In addition, the *FLAC3D*  
496 model simulates all of the processes related to in situ stress through the application of  
497 horizontal strain acting on linear elastic materials, although it is clear that many other  
498 processes such as glaciotectionics and geological history are major factors. In addition, the  
499 model does not account for the effects of large- or small-scale structural geology. Some of  
500 the units are particularly weak and/or prone to long-term creep (i.e., time-dependent shear  
501 strain under constant load), such as the evaporite rocks in the Salina Formation. For these  
502 rocks, creep over geological time scales would likely reduce the in situ stress ratios from  
503 those induced by tectonic strain to values near  $K_H = K_h = 1$  [30].

## 504 **6.0 Conclusions**

505 To assess the performance and the design of an underground repository, an estimation  
506 of in situ stress representative of the site is a necessity, in particular the horizontal  
507 components. This is typically challenging using surface-based investigation programs.  
508 Literature-reported stress gradients are generally adequate only for the task of preliminary  
509 or scoping analysis. However, in a horizontally layered sedimentary sequence of shales  
510 and carbonates where the stiffness contrasts of discrete rock units exist, a simple approach

511 of modelling horizontal ground stresses in the discrete rock units responding to tectonic  
512 strains has been proposed to capture the complexity of sedimentary profiles. This approach  
513 increases confidence in the estimation of horizontal in situ stresses by incorporating site  
514 specific information that has not been accounted for in past evaluations of regional stresses.

515 This paper described the use of simplified three-dimensional finite difference  
516 modelling (*FLAC3D*) to simulate the regional tectonic strain through the full stratigraphic  
517 section of interest for the DGR project site consisting of a sedimentary sequence of discrete  
518 rock unit with contrasting stiffness. The model was calibrated with tectonic strain deduced  
519 from in situ stress measurements from Norton Mine, where similar lithological conditions  
520 exist, and from DGR site-specific borehole information. The calibrated model agreed well  
521 with literature-reported values, field measurements and observations while capturing the  
522 impact of discrete rock unit stiffness. This is particularly important for long-term  
523 evaluation of shaft performance (e.g., shaft seals).

524 Although the model-predicted in situ stress profile represents an improvement over  
525 information provided in historical literature, it would require validation by a site-specific  
526 in situ stress measurement program. For the DGR project, ground stress tensors in the host  
527 and other selected formations will be verified by performing mine-by instrumented  
528 excavation type experiments during repository lateral development and by overcoring  
529 stress measurements during shaft sinking, respectively [2]. Future work may also account  
530 for the anisotropic stiffness of the horizontally layered sedimentary rocks and perhaps long-  
531 term creep, especially in the evaporite units, which could have significant effect on stress  
532 estimation. However, given the typical high range of uncertainty related to in situ stress  
533 determination programs, and the lack of any site-specific measurements, the model-  
534 predicted horizontal stresses offer a significantly improved estimate for the performance  
535 assessment of the proposed DGR shaft.

## 536 **Acknowledgements**

537 The authors would like to thank NWMO for permission to publish this work and  
538 specifically Mark Jensen for his review comments. Several engineers and support staff at  
539 Itasca Consulting Group, Inc. provided valuable assistance during the project. Helpful  
540 advice and review was provided by the DGR Project's Geomechanics Review Committee:

541 Mark Diederichs, Derek Martin and Dougal McCreath. Judy MacLean kindly assisted with  
542 editing the manuscript.

## 543 **References**

544 [1] Intera. Descriptive Geosphere Site Model. Intera Engineering Ltd report for the  
545 Nuclear Waste Management Organization NWMO DGR-TR-2011-24 R000 2011.

546 [2] NWMO. Geoscientific Verification Plan, Nuclear Waste Management  
547 Organization Technical Report. NWMO DGR-TR-2011-38-R001 2014.

548 [3] Amadei B, Swolfs HS, Savage WZ. Gravity-induced stresses in stratified rock  
549 masses. *Rock Mech Rock Eng* 1988; 21:1-20.

550 [4] Esterhuizen E, Mark C, Murphy MM. Numerical model calibration for simulating  
551 coal pillars, gob and overburden response. *Proceedings: International Conference on*  
552 *Ground Control in Mining ICGCM 2010:46-57.*

553 [5] Evans K, Engelder T. Some problems in estimating horizontal stress magnitudes  
554 in “thrust” regimes. *Int J Rock Mech Min Sci* 1989; 26:647-60.

555 [6] Adams J, Bell JS. Crustal Stresses in Canada. In: Zoback MD, Blackwell DD,  
556 editors. *Neotectonics of North America: Geological Society of America*; 1991, p. 367-  
557 386.

558 [7] Lam T, Martin D, McCreath DR. Characterising the geomechanics properties of  
559 the sedimentary rocks for the DGR excavations. *Canadian Geotechnical Conference*  
560 *OttawaGeo2007 2007:636-44.*

561 [8] Kaiser PK, Maloney S. Review of Ground Stress Database for the Canadian  
562 Shield. Report to Ontario Power Generation, MIRARCO Mining Innovation Report No:  
563 06819-REP-01300-10107-R00 2005.

564 [9] Haimson BC. Michigan Basin Deep Borehole. *J Geophys* 1978:5857-63.

565 [10] Damjanac B. Long-Term Geomechanical Stability Analysis, OPG's Deep  
566 Geological Repository for Low & Intermediate Waste, Itasca Consulting Group, Inc.  
567 report for the Nuclear Waste Management Organization NWMO DGR-TR-2011-17  
568 R000.Toronto, Canada. 2011.

569 [11] Itasca Consulting Group Inc. *FLAC3D* (Fast Lagrangian Analysis of a Continua  
570 in 3 Dimensions) User's Manual. 2005; Version 3.1.

571 [12] Valley B, Maloney S. Analyses of DGR-1 and DGR-2 Borehole Images for  
572 Stress Characterization, Report to Ontario Power Generation, Intera Engineering Ltd.  
573 2009.

574 [13] Dineva S, Eaton D, Mereu R. Seismicity of the southern Great Lakes: Revised  
575 earthquake hypocenters and possible tectonic controls. *Bull Seismol Soc Am* 2004;  
576 94:1902-18.

577 [14] Haimson BC, Lee CF. Hydrofracturing stress determinations at Darlington,  
578 Ontario. 13th Canadian Rock Mechanics Symposium 1980.

579 [15] Yong S, Maloney S. An Update to the Canadian Shield Stress Database.  
580 MIRARCO report to NWMO TR-2015-18 2015.

581 [16] Arjang B. Database on Canadian In Situ Ground Stresses, CANMET Mining and  
582 Mineral Sciences Laboratories report. 2001.

583 [17] Martin CD, Kaiser PK, Christiansson R. Stress, instability and design of  
584 underground excavations. *Int J Rock Mech Min Sci* 2003; 40:1027-47.

585 [18] Heidbach O, Tingay M, Barth A, Reinecker J, Kurfess J, Muller B. World Stress  
586 Map database release 2008.

587 [19] Bauer SJ, Munson DE, Hardy MP, Barrix J, McGunegle B. In Situ Stress  
588 Measurements and Their Implications in a Deep Ohio Mine. *Alaska Rocks* 2005, The  
589 40th US Symposium on Rock Mechanics (USRMS) 2005.

- 590 [20] Brown ET, Hoek E. Trends in relationships between measured rock in situ  
591 stresses and depth. *Int J Rock Mech Min Sci* 1978; 15:211-5.
- 592 [21] Herget G. *Stresses in Rock*. Rotterdam: Balkema, 1988.
- 593 [22] Sheorey PR. A theory for in situ stresses in isotropic and transversely isotropic  
594 rock. *Int J Rock Mech Min Sci* 1994; 31:23-34.
- 595 [23] Swolfs HS. *The Triangular Stress Diagram: A Graphical Representation of*  
596 *Crustal Stress Measurements*, Geological Survey Professional Paper 1291, U.S.  
597 Department of the Interior. 1984.
- 598 [24] Zoback M. Determination of stress orientation and magnitude in deep wells. *Int J*  
599 *Rock Mech Min Sci* 2003; 40:1049-76.
- 600 [25] Brace WF, Martin RJ. A test of the law of effective stress for crystalline rocks of  
601 low porosity. *Int J Rock Mech Min Sci* 1968; 5:415-26.
- 602 [26] Martin CD. Seventeenth Canadian Geotechnical Colloquium: the effect of  
603 cohesion loss and stress path on brittle rock strength. *Can Geotech J* 1997; 34:698-725.
- 604 [27] Hoek E, Martin CD. Fracture initiation and propagation in intact rock - A  
605 review. *J Rock Mech Geotech Eng* 2014; 6:287-300.
- 606 [28] Hatch Limited. OPG's Deep Geological Repository for Low and Intermediate  
607 Level Waste: Conceptual Design Report, Report to Ontario Power Generation. 2008.
- 608 [29] Damjanac B, Fairhurst C. Evidence for a Long-Term Strength Threshold in  
609 Crystalline Rock. *Rock Mech Rock Eng* 2010; 43:513-31.
- 610 [30] Eriksson LG, Michalski A. Hydrostatic conditions in salt domes - a reality or a  
611 modeling simplification. 1986:121-32.

612 [31] Jensen M, Lam T, Luhowy D, Mclay J, Semec B, Frizzell R. Ontario Power  
613 Generations Proposed L and ILW Deep Geologic Repository: An Overview of  
614 Geoscientific Studies. Canadian Geotechnical Conference, Halifax 2008:1339-47.

615 [32] Mazurak M. Long Term Nuclear Waste Management - Geoscientific Review of  
616 the Sedimentary Sequence in Southern Ontario. 2004.

617



## TABLE CAPTIONS

618

619

620 **Table 1.** Constraints on stress magnitudes given by borehole televiewer log observations  
621 using  $\sigma_{ci} = 0.5 \sigma_c$  and  $\sigma_t = 0$  as compressive and tensile strength criteria, respectively.

622

623 **Table 2.** Stratigraphic Units corresponding elastic properties comprising the  
624 Geotechnical Model. [These Unit numbers are shown on Fig. 3.](#)

625

626 **Table 3.** Formations and stress conditions at the Access Shaft seal locations for preliminary  
627 design purposes [10].

628

## FIGURE CAPTIONS

629

630

631 **Fig. 1.** Conceptual illustration of proposed DGR project at the Bruce Nuclear Site (after  
632 [31]).

633

634 **Fig. 2.** Regional geological basins in the DGR project area (modified after [32]).

635

636 **Fig. 3.** Bedrock stratigraphy at the proposed DGR site based on boreholes DGR-1 and  
637 DGR-2 (after [7]). The Stratigraphic Unit numbers (circled) corresponding to those in  
638 Table 2 are shown.

639

640 **Fig. 4.** Stress measurements and indicators in Southern Ontario and Mid-Western U.S.  
641 from the World Stress Map Project (modified after [32]).

642

643 **Fig. 5.** Literature-reported in situ stress gradients for Southern-Ontario for the full depth  
644 of the proposed DGR Access Shaft.

645

646 **Fig. 6.** Horizontal in situ stress constraints from borehole televiewer observations. (a)  
647 Markers indicate the maximum value of  $\sigma_H$ . (b) Markers indicate the minimum value of  
648  $\sigma_h$ .

649

650 **Fig. 7.** DGR borehole long axis orientation histograms for Middle Ordovician formations.  
651 (a) DGR-1 and DGR-2; (b) DGR-3; and (c) DGR-4. Peak values are interpreted to  
652 indicate the orientation of the minimum horizontal in situ stress for all orientations (upper  
653 region with vertical lines) and for axis ratios greater than 1.0025 (lower solid region).

654

655 **Fig. 8.** Conceptual schematic showing the setup of the single-zone-wide *FLAC3D* model.  
656 The model extends through the full vertical stratigraphy of the proposed DGR Access  
657 Shaft. The model was deformed at a constant x- and y-velocity ratio to simulate tectonic  
658 strain (indicated by arrows) resulting in stress variations relative to the stiffness of the  
659 various units.

660

661 **Fig. 9.** Profile of horizontal stresses from the calibrated *FLAC3D* in situ stress model  
662 compared with constraints (borehole and Norton Mine measured values) and literature-  
663 reported gradients.

664

665 **Fig. 10.** Model-predicted horizontal stress ratios. The results are similar to those reported  
666 by Sheorey [22].

667

668 **Fig. 11.** Model-predicted  $\sigma_{max}$  compared with values calculated from literature-reported  
669 stress gradients. The parameter  $\sigma_{max}$  is an important indicator of short- and long-term shaft  
670 performance.

671

## Figures

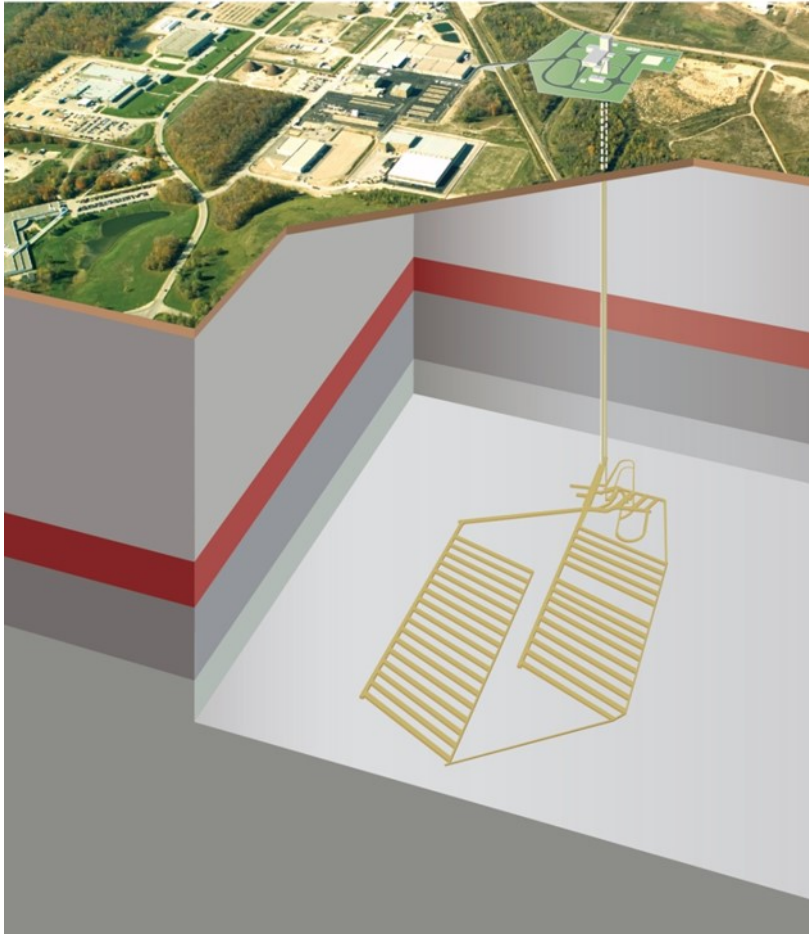


Figure 1

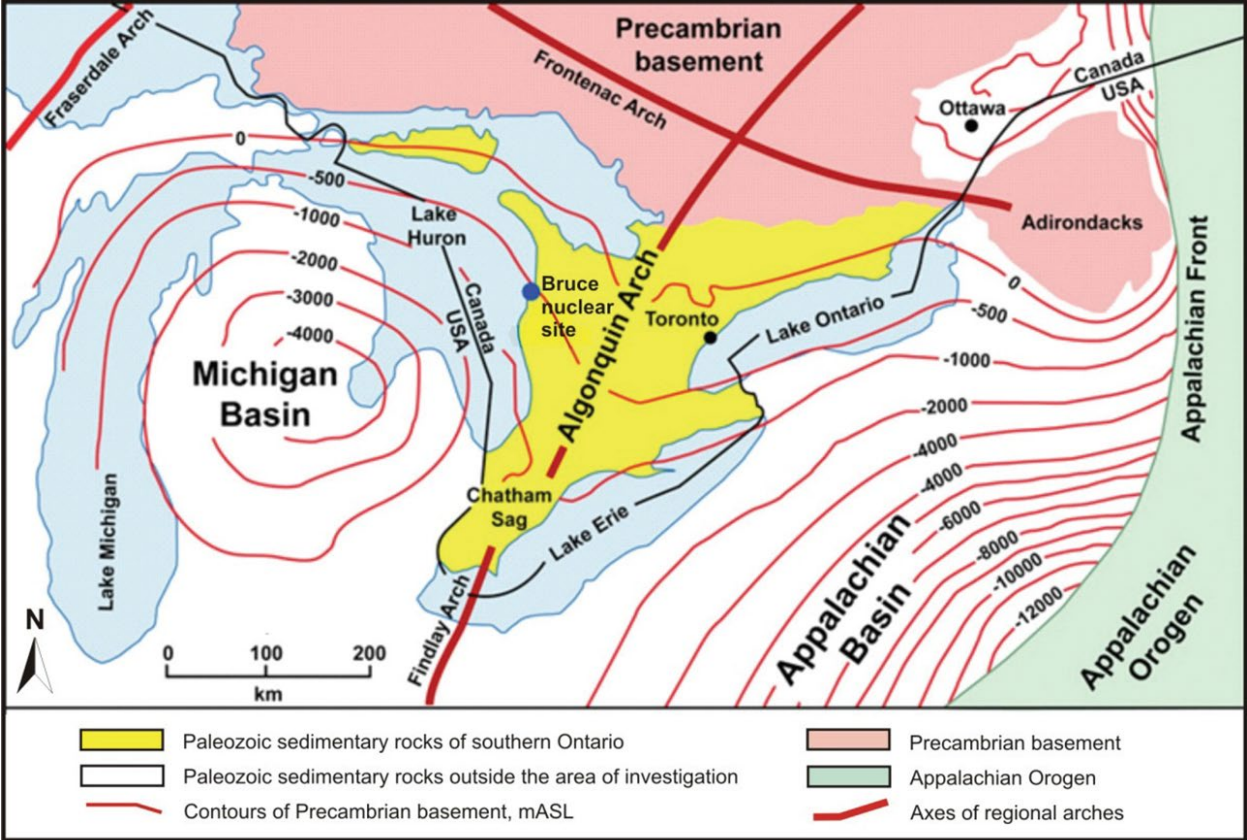


Figure 2

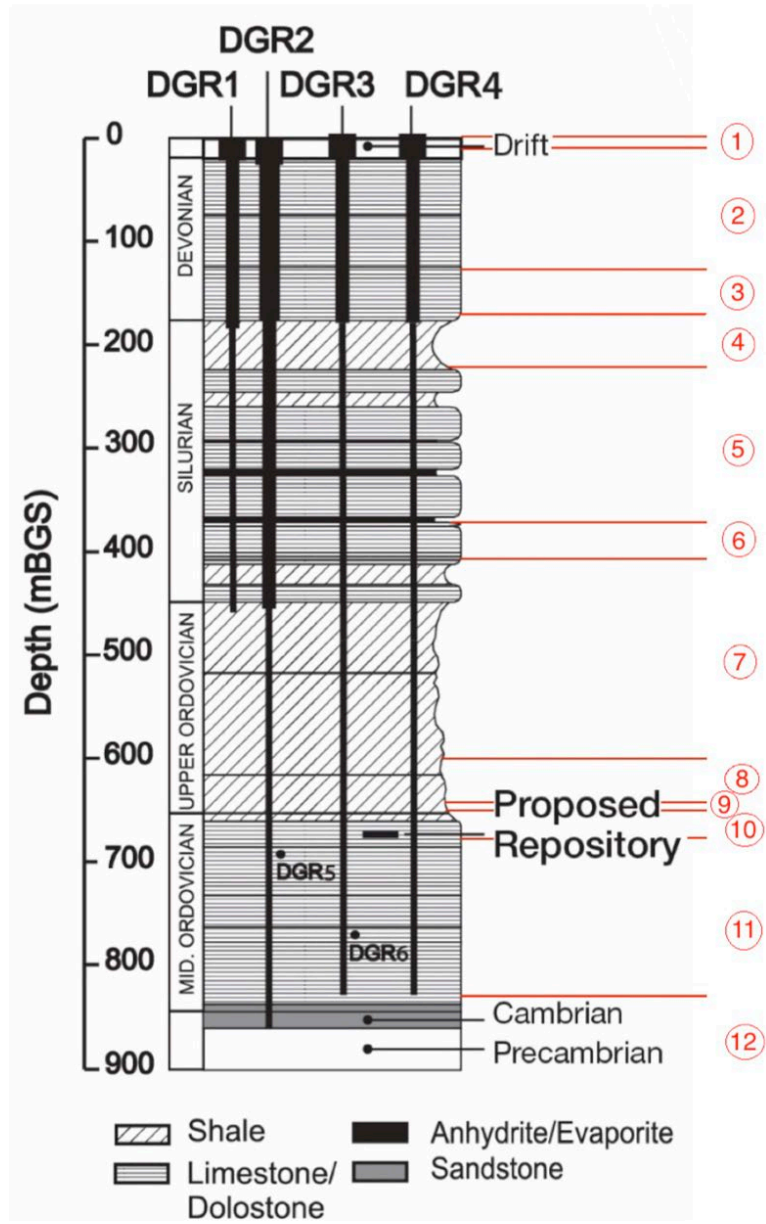


Figure 3

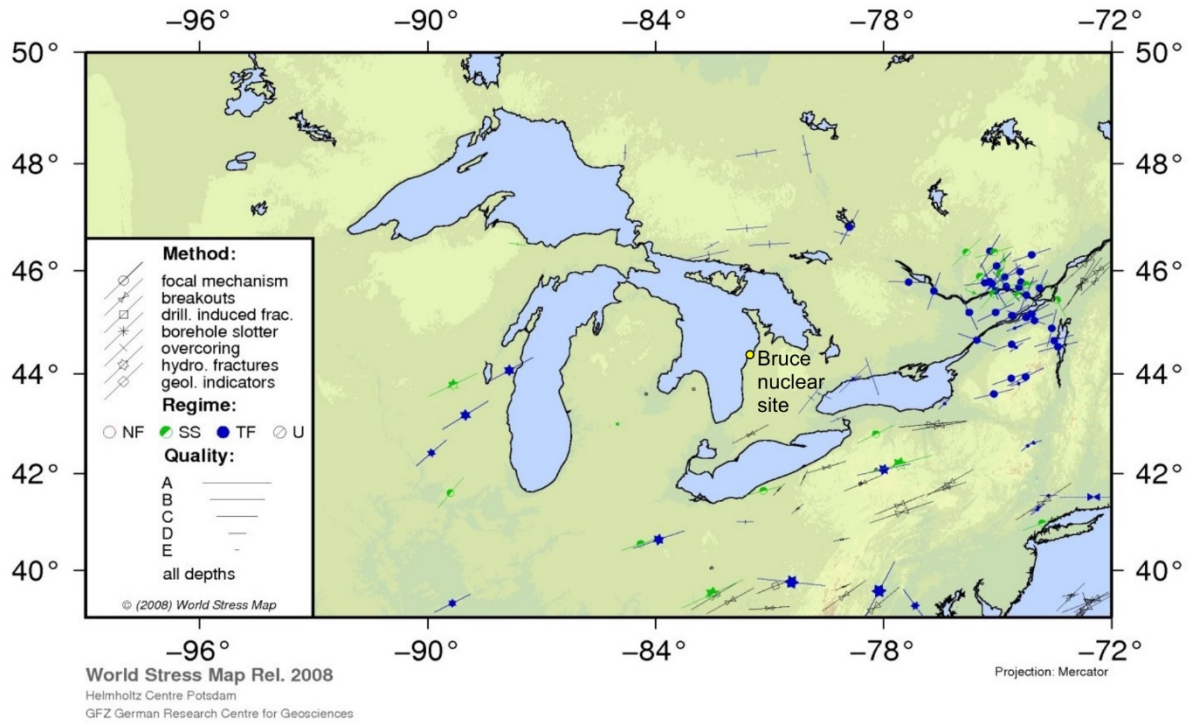


Figure 4



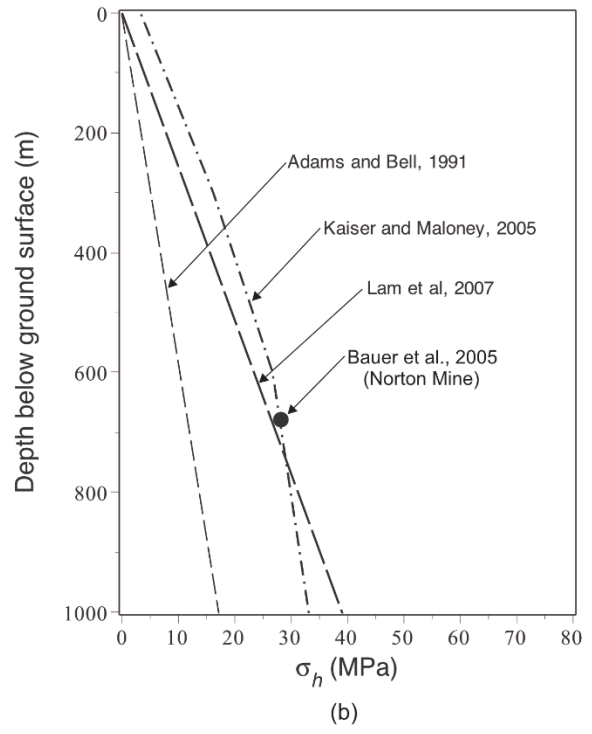
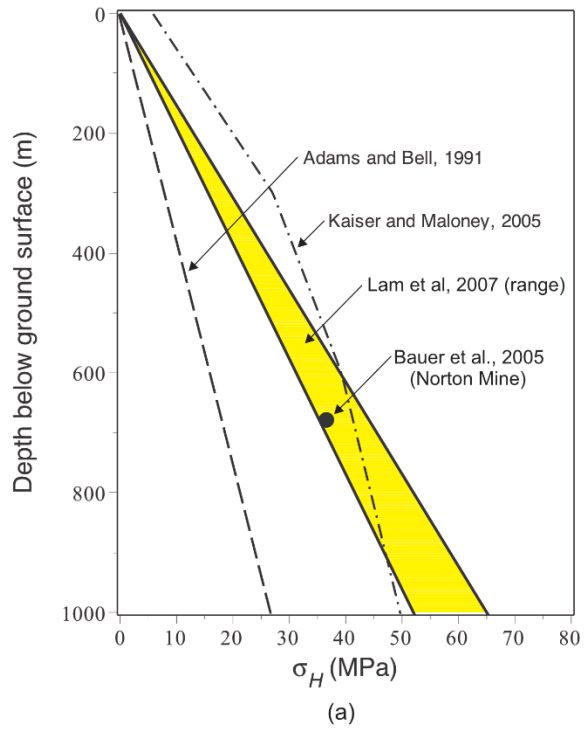


Figure 5

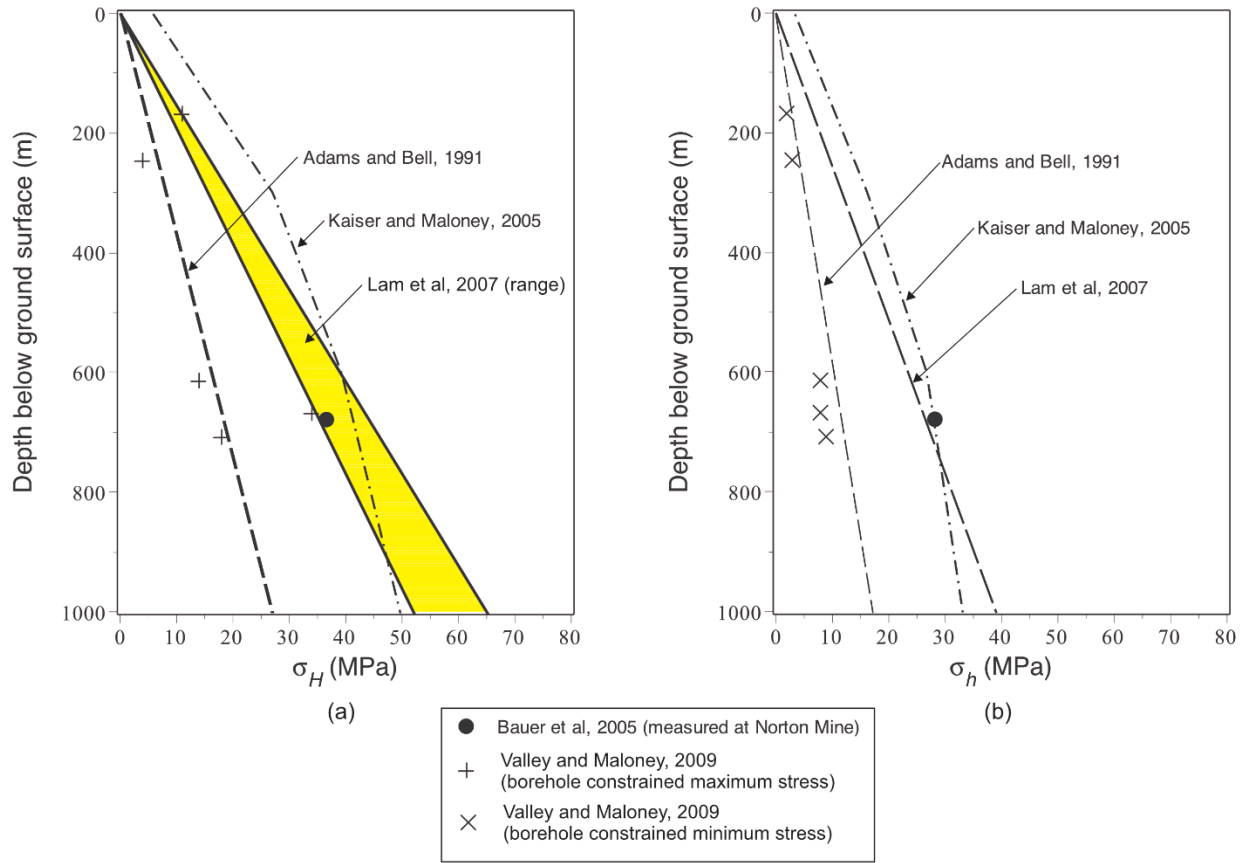


Figure 6

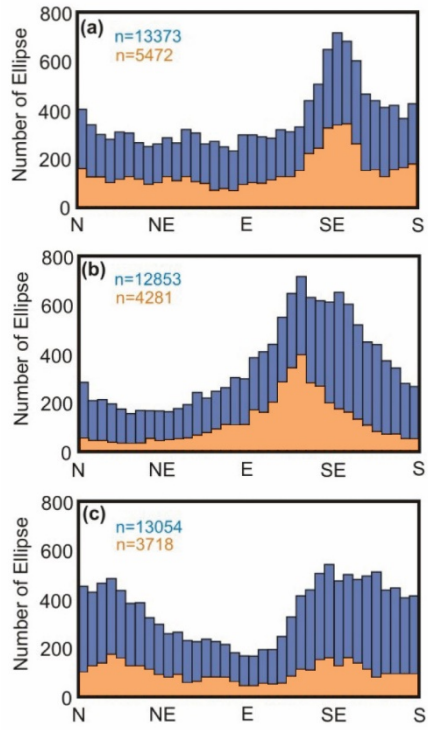


Figure 7

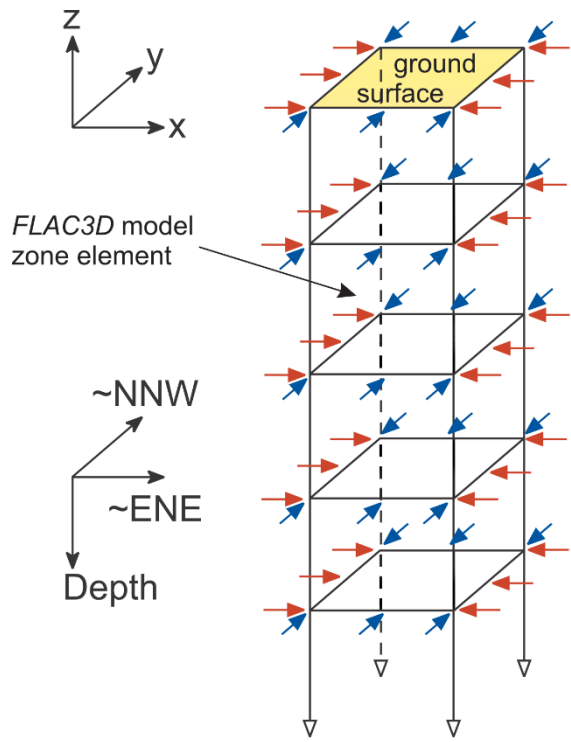


Figure 8

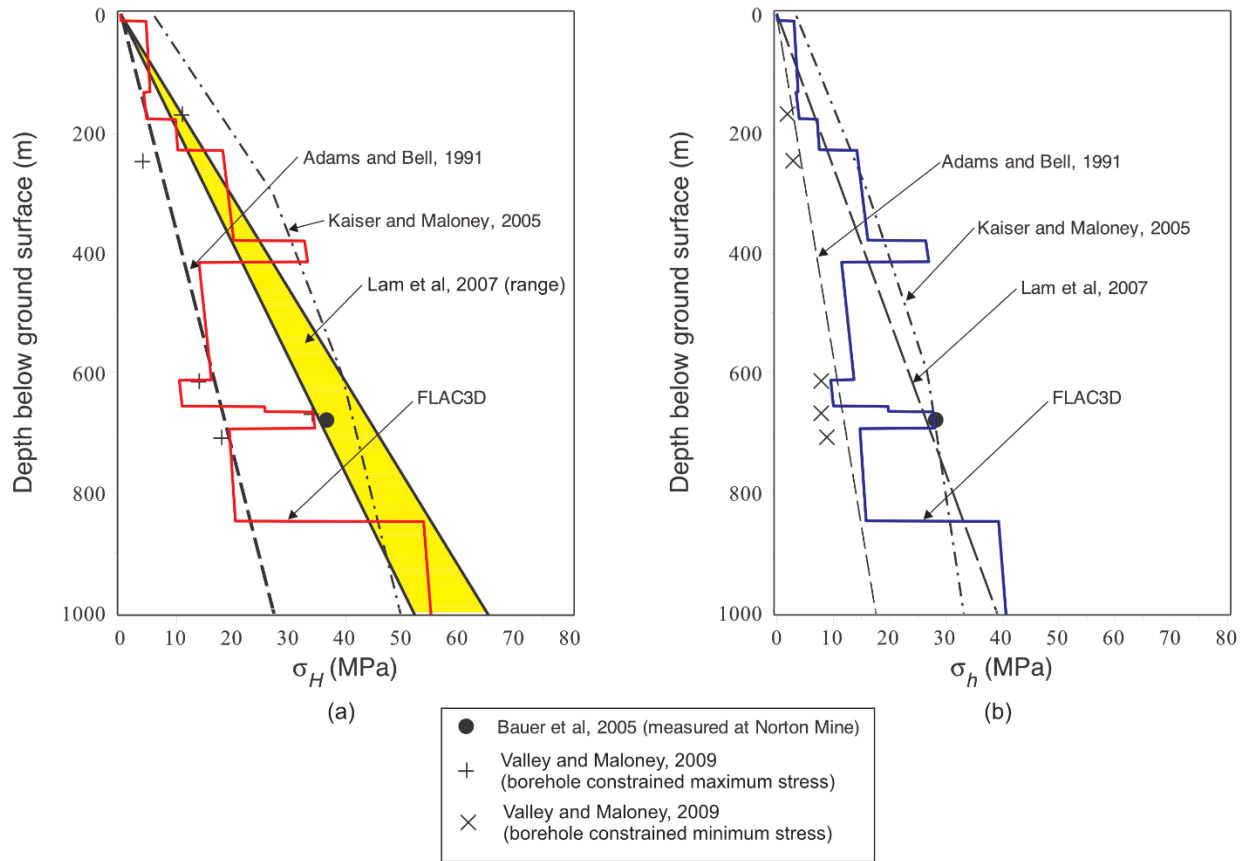


Figure 9

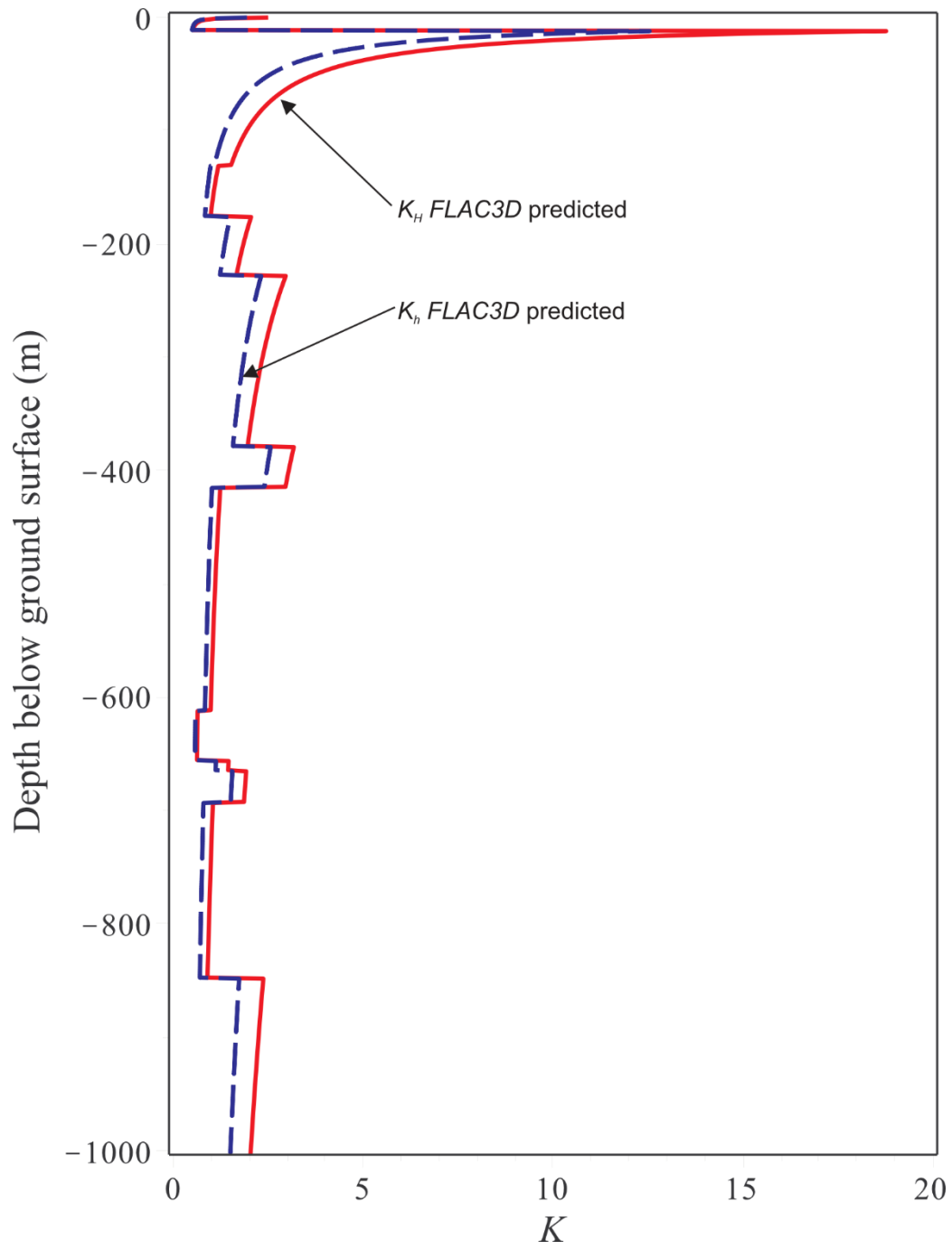


Figure 10

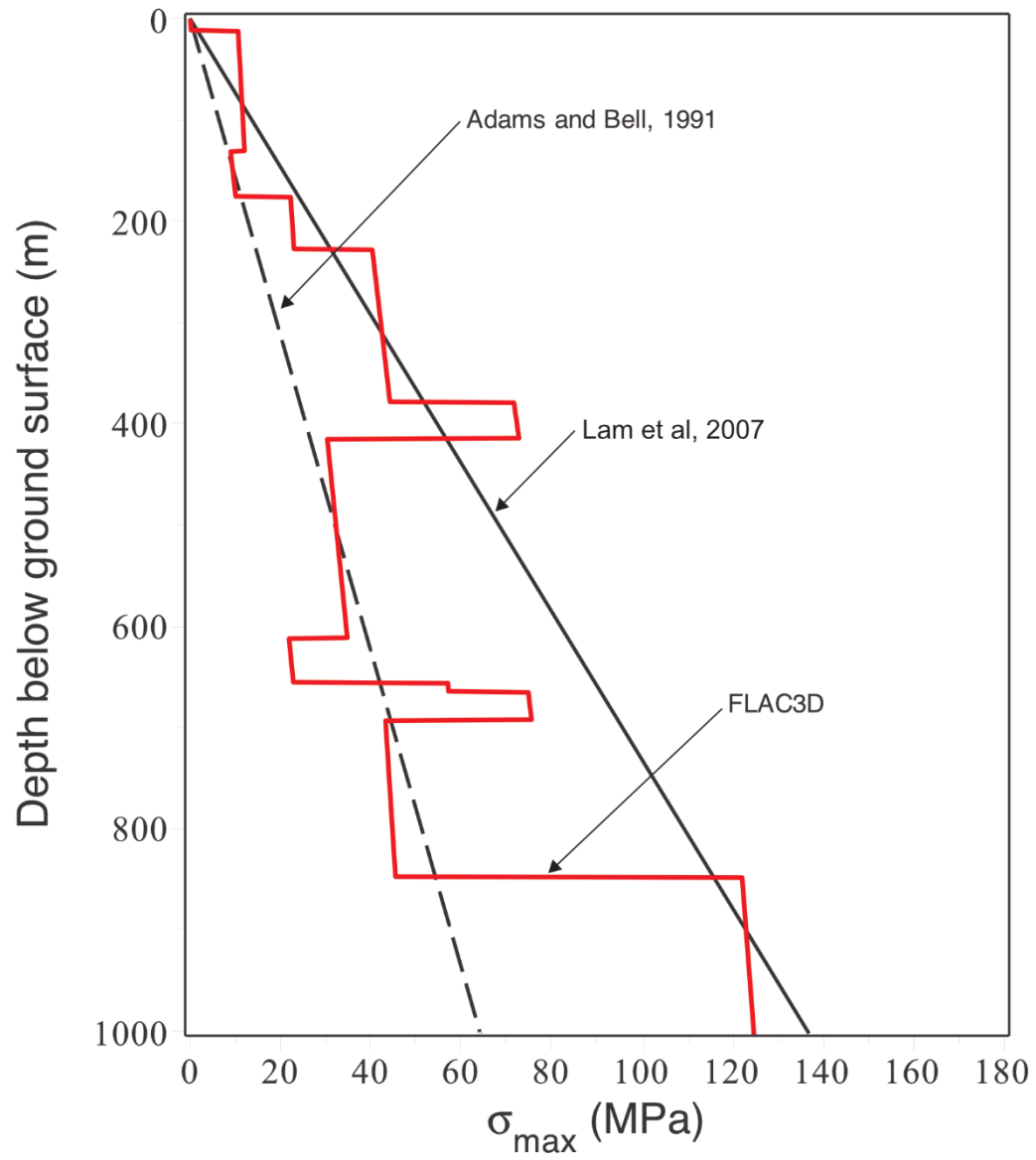


Figure 11